Dramatic Raman Gain Suppression in the Vicinity of the Zero Dispersion Point in a Gas-Filled Hollow-Core Photonic Crystal Fiber

S. T. Bauerschmidt,[1] D. Novoa,[1] and P. St. J. Russell[1,2]
[1]Max Planck Institute for the Science of Light, Guenther-Scharowsky-Strasse 1, 91058 Erlangen, Germany
[2]Department of Physics, University of Erlangen-Nuremberg, 91058 Erlangen, Germany
(Received 25 August 2015; published 11 December 2015)

In 1964 Bloembergen and Shen predicted that Raman gain could be suppressed if the rates of phonon creation and annihilation (by inelastic scattering) exactly balance. This is only possible if the momentum required for each process is identical, i.e., phonon coherence waves created by pump-to-Stokes scattering are identical to those annihilated in pump-to-anti-Stokes scattering. In bulk gas cells, this can only be achieved over limited interaction lengths at an oblique angle to the pump axis. Here we report a simple system that provides dramatic Raman gain suppression over long collinear path lengths in hydrogen. It consists of a gas-filled hollow-core photonic crystal fiber whose zero dispersion point is pressure adjusted to lie close to the pump laser wavelength. At a certain precise pressure, stimulated generation of Stokes light in the fundamental mode is completely suppressed, allowing other much weaker phenomena such as spontaneous Raman scattering to be explored at high pump powers.

DOI: 10.1103/PhysRevLett.115.243901 PACS numbers: 42.65.Dr, 42.65.Ky, 42.81.-i

When a laser pump beam propagates in a Raman active medium, a Stokes signal, down-shifted by the transition frequency Ω_R of the Raman-active molecules, is usually generated [1]. This process is initiated from noise in the form of thermally excited molecular vibrations or vacuum fluctuations. Beating between pump and Stokes signals creates a pattern of fringes moving at the group velocity of the light. This fringe pattern drives the generation of a strong coherence wave of synchronized molecular vibrations that further enhances scattering into the Stokes band. The resulting cycle of cause and effect results in exponential growth of the Stokes signal. Under some circumstances, the coherence wave can also cause up-conversion of pump photons to the anti-Stokes frequency, a process that results in phonon annihilation. The efficiency of this process depends strongly on the optical dispersion: if the coherence wave created in pump-to-Stokes conversion is identical to the one annihilated in pump-to-anti-Stokes conversion (this would occur, for example, when the chromatic dispersion is zero), then the rates of phonon creation and annihilation precisely balance, resulting in perfect suppression of the Raman gain and therefore negligible growth of the Stokes signal above the noise level. This effect was first predicted by Bloembergen and Shen in 1964 [2] for the steady state regime and later by different groups also for the transient regime [3–5].

In free space configurations involving bulk media or gases, the chromatic dispersion is nonzero, making gain suppression difficult to achieve. Indeed, the only experimental evidence of gain suppression to date is the observation of a dark ring in the emission cone of the anti-Stokes signal in a gas cell [6].

In this Letter, we report dramatic Raman gain suppression in a collinear geometry involving a hydrogen-filled hollow-core photonic crystal fiber (PCF). Hollow-core PCF [7] has in recent years emerged as an ideal vehicle for enhancing gas-based nonlinear optics. This is because it offers tight modal confinement, long well-controlled interaction lengths, a very high damage threshold, and precise pressure control of the dispersion and nonlinearity [8,9]. Broadband-guiding kagome-style hollow-core PCF in particular, when filled with gases or vapors, has proven highly effective in Raman-related wavelength conversion [9–11], Cs-based quantum memories [12], frequency combs [13], and supercontinuum generation [14].

Recently, it was shown that the unique S-shaped dispersion curve in the vicinity of the pressure-tunable zero dispersion point (ZDP) in hydrogen-filled kagome PCF permits the coherence wave created by pump-to-Stokes scattering (from ω_{p1} to $\omega_{p1}-\Omega_R$, where $\Omega_R/2\pi$ is the Raman frequency) to be used to achieve perfectly phase-matched anti-Stokes scattering from a widely different pump frequency, i.e., from ω_{p2} to $\omega_{p2}+\Omega_R$ [11]. Here, we show that by an appropriate choice of pressure, ω_{p1} can be arranged to be identical with ω_{p2}, creating the conditions for Raman gain suppression. If this condition is not perfectly fulfilled, as is normally the case in stimulated Raman scattering (SRS), the Stokes signal is amplified above the threshold according to $I_{s0}\exp(\gamma_{\mathrm{eff}} I_p z)$, where γ_{eff} is the effective Raman gain, z the propagation distance, I_p the pump intensity, and I_{s0} the initial value of the Stokes intensity.

The effective gain may be written in the form

$$\gamma_{\mathrm{eff}} = \rho S_{ij} g_P, \tag{1}$$

where S_{ij} is the spatial overlap integral between the LP_{01} pump and the LP_{ij} Stokes mode, g_p is the Raman gain of the gas, and ρ is the gain reduction factor, which for no pump depletion and negligible Kerr nonlinearity can be expressed in the form [1,15]

$$\rho = \left| \mathrm{Re}\sqrt{\left(\frac{p-1}{2}\right)^2 - \left(\frac{\vartheta_{01}}{g_P I_P}\right)^2 - i(p+1)\frac{\vartheta_{01}}{g_P I_P}} \right| - \left(\frac{p-1}{2}\right), \quad (2)$$

where $p = g_{AS}\omega_{AS}/(g_P\omega_P) > 1$ and g_i is the Raman gain at pump frequency ω_i. Gain suppression (i.e., $\rho = 0$) occurs when the dephasing parameter $\vartheta_{01} = \beta_{01}(\omega_{AS}) + \beta_{01}(\omega_S) - 2\beta_{01}(\omega_P)$ is zero [2–5], where $\beta_{ij}(\omega)$ is the propagation constant of the LP_{ij} mode at frequency ω. In a kagome PCF, $\beta_{ij}(\omega)$ can be approximated to good accuracy by

$$\beta_{ij} = \sqrt{k_0^2 n_{gas}^2(p,\lambda) - u_{ij}^2/a^2(\lambda)}, \quad (3)$$

where $k_0 = 2\pi/\lambda$ is the vacuum wave vector, n_{gas} the refractive index of the filling gas, p the gas pressure, u_{ij} the jth root of the ith order Bessel function of the first kind, and $a(\lambda) = a_{AP}[1 + t\lambda^2/(a_{AP}d)]$, where a_{AP} is the area-preserving core radius, $t = 0.06$ is an empirical parameter derived from finite element modeling of an idealized kagome structure, and d is the core wall thickness [16].

Since ϑ_{01} depends directly on gas pressure [11], precise tuning of the gain suppression point is possible without the need for the complicated crossed-beam arrangements used in free space configurations. Pressure adjustment of phase-matching conditions has been previously employed, e.g., in high-harmonic generation in hollow capillaries, although not in the vicinity of the ZDP [17]. Although coherent Raman gain suppression has been studied in solid core fibers, it is severely impaired by four-wave mixing and by the broadband nature of the Raman gain which, together with strong higher order dispersion, restricts perfect gain suppression to a narrow portion of the Stokes gain band [18,19]. There are other approaches to accomplishing Raman gain suppression without resorting to coherent effects, for example, using an all-solid photonic band-gap fiber where the threshold for SRS is increased by the large attenuation experienced by the Stokes signal when it is located outside the guidance band [20].

The gain reduction factor ρ is plotted in Fig. 1 against $(\vartheta_{01}/g_P I_P)$ for $p = 1.87$, measured experimentally via the Raman gain [21]. Note that $S_{01} = 1$ since all the signals are in the LP_{01} mode.

The LP_{01} dispersion curve for perfect gain suppression is shown in Fig. 2, for a kagome PCF with a 30 μm core diameter filled with hydrogen at 24.7 bar. The Raman frequency shift is $\Omega_R/2\pi \approx 125$ THz, which corresponds to the fundamental vibrational mode of hydrogen. Perfect gain suppression is expected for a pump signal at 683 nm, which is very close to the ZDP at 698 nm. Under these conditions the phonon four vectors (indicated by green dashed lines) for pump-to-Stokes and pump-to-anti-Stokes scattering in the LP_{01} mode are identical.

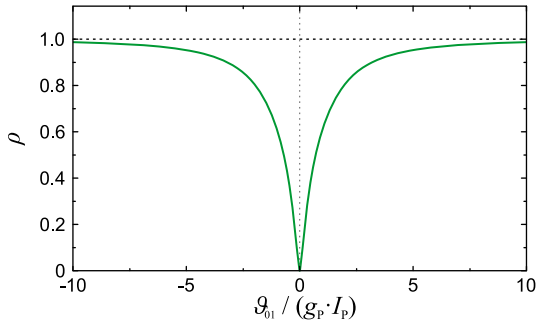

FIG. 1 (color online). The gain reduction factor ρ is plotted against the normalized dephasing parameter $(\vartheta_{01}/g_P I_P)$.

To demonstrate gain suppression experimentally, a 90 cm long hydrogen-filled kagome PCF with 30 μm core diameter was pumped with 1.6 ns, 2.5 μJ laser pulses at 683 nm (Fig. 3). These pulses were generated via SRS from a 532 nm laser in a second length of hydrogen-filled kagome PCF. The output spectrum was monitored with an optical spectrum analyzer and the near-field profiles of the modes imaged at the fiber end face using a CCD camera [see Figs. 4(a,b)].

The photon flux (i.e., the number per second) in the three signals at the fiber output was recorded while scanning the hydrogen-filling pressure [see Fig. 4(b)]. Although the Stokes signal at 955 nm dropped by about 10 dB in the vicinity of the calculated gain suppression pressure, it did not completely disappear as expected. Strong suppression was, however, clearly apparent in the anti-Stokes signal at

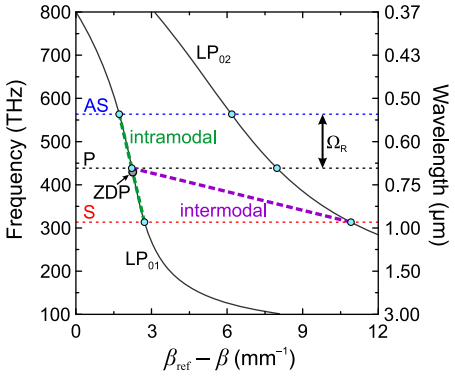

FIG. 2 (color online). Dispersion diagram for a kagome PCF at a hydrogen-filling pressure of 24.7 bar. Dispersion curves for the LP_{01} and LP_{02} mode are shown. In order to magnify the small but crucial deviation from an ideal linear dispersion relation, we plot against $(\beta_{ref} - \beta)$, where β_{ref} is a linear function of frequency chosen such that $(\beta_{ref} - \beta_{01})$ is zero at 800 THz.

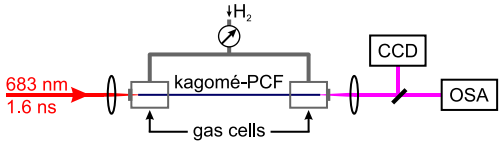

FIG. 3 (color online). Sketch of the experimental setup. OSA, Optical spectrum analyzer; CCD, camera.

532 nm, which vanished at this pressure. It turned out that the Stokes signal exactly at the gain suppression point was in the LP_{02} mode, the LP_{01} mode having been completely suppressed. Tuning the pressure away from this point, the Stokes light underwent a smooth transition from the LP_{02} to the LP_{01} mode [see Fig. 4(a)]. Stokes emission into the LP_{02} mode occurs via the intermodal coherence wave marked in Fig. 2 by the purple dashed line. It turns out that the intermodal overlap (and hence the gain) is larger for the LP_{02} mode ($S_{02} = 0.85$) than for any other higher order mode. As a result, when the LP_{01} gain is suppressed, the LP_{02} mode is the first to appear because its net gain (taking account of gain and loss) is the highest of any of the higher order modes [see gray-shaded region in Fig. 4(b)]. Conversely, the anti-Stokes signal was always observed in a pure LP_{01} mode. This is because scattering to the LP_{02} anti-Stokes band is inhibited by the lack of LP_{02} pump light and strong dephasing of the available intermodal transitions.

To model the system in the gain suppression region, we used a semiclassical treatment of SRS [22] based on a multimode-extended set of coupled Maxwell-Bloch equations, namely

$$\frac{\partial}{\partial z}E_{\sigma,l} = -\kappa_{2,l}\frac{\omega_l}{\omega_{l-1}}\sum_{\nu\xi\eta}^{M} i\frac{s_{\sigma\nu\xi\eta}}{s_{\nu\xi}}Q_{\nu\xi}E_{\eta,l-1}q_{\eta,l-1}q^*_{\sigma,l} - \kappa_{2,l+1}\sum_{\nu\xi\eta}^{M} i\frac{s_{\sigma\nu\xi\eta}}{s_{\nu\xi}}Q^*_{\nu\xi}E_{\eta,l+1}q_{\eta,l+1}q^*_{\sigma,l} - \frac{1}{2}\alpha_{\sigma,l}E_{\sigma,l}, \quad (4)$$

$$\frac{\partial}{\partial\tau}Q_{\nu\xi} = -Q_{\nu\xi}/T_2 + in\frac{1}{4}s_{\nu\xi}\sum_l \kappa_{1,l}E_{\nu,l}E^*_{\xi,l-1}q_{\nu,l}q^*_{\xi,l-1}, \quad (5)$$

where the integer l denotes the sideband at frequency $\omega_l = \omega_P + l\Omega$ and the summations go over all possible permutations of the modal set M. We describe the complex electric field amplitude $e_{\sigma,l}(x,y,z,\tau) = F_\sigma(x,y)E_{\sigma,l}(z,\tau)q_{\sigma,l}$ of a guided mode (mode index σ) in terms of its normalized transverse spatial profile $F_\sigma(x,y)$, the slowly varying field envelope $E_{\sigma,l}(z,\tau)$, and the fast oscillating phase term $q_{\sigma,l} = \exp[-i\beta_\sigma(\omega_l)z]$. Q is the Raman coherence and τ is the time relative to a frame traveling with the group velocity of the pump pulse. The coupling constants $\kappa_{1,l} = c\varepsilon_0[2g_l/(NT_2\hbar\omega_{l-1})]^{0.5}$ and $\kappa_{2,l} = \kappa_{1,l}N\hbar\omega_{l-1}/(2c\varepsilon_0)$ can be derived from experimentally measured gain values g_l [21], where N is the molecular number density, c the vacuum speed of light, $\hbar$ the reduced Planck's constant, ε_0 the vacuum permittivity, and T_2 the dephasing time of the

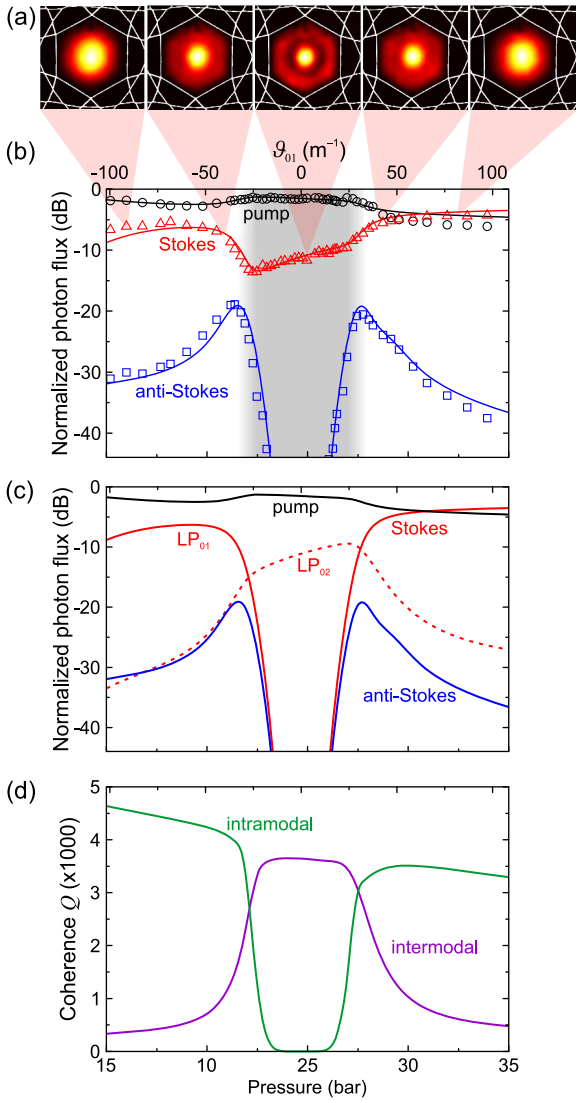

FIG. 4 (color online). (a) Near-field profiles of the Stokes light at the fiber end face recorded at the different pressures and overlaid onto a scanning electron micrograph of the fiber microstructure. (b) Measured (symbols) and simulated (solid lines) photon flux (number per second) in the pump, Stokes, and anti-Stokes bands, plotted against increasing pressure and normalized to the launched flux of pump photons. Stokes light is emitted in the LP_{02} mode within the gray-shaded region. (c) Simulated photon flux of pump, Stokes, and anti-Stokes bands in the LP_{01} (solid lines) and LP_{02} (dashed line) mode plotted against increasing pressure and normalized to the launched pump signal. (d) Simulated maximum value of intramodal and intermodal coherence Q plotted against increasing pressure.

Raman coherence [21]. Since the highest coherence achieved in the experiment is of the order of 0.001, the population imbalance n is assumed to be -1; i.e., the majority of the hydrogen molecules remain in the ground state.

The generalized nonlinear spatial overlap integrals are given by [23]

$$s_{\sigma\nu\xi\eta} = \frac{\int F_\sigma^* F_\nu^* F_\xi F_\eta dA}{(\int |F_\sigma|^2 dA \int |F_\nu|^2 dA \int |F_\xi|^2 dA \int |F_\eta|^2 dA)^{1/2}} A_{\text{eff}} \tag{6}$$

and

$$s_{\nu\xi} = \frac{\int |F_\nu|^2 |F_\xi|^2 dA}{(\int |F_\nu||F_\xi| dA)^2} A_{\text{eff}}, \tag{7}$$

where A_{eff} is the effective mode area of the pump in the fundamental mode [24] and the integrals are evaluated over the transverse cross section of the fiber. The transverse mode field profiles $F_\sigma(x, y)$ are obtained via finite element modeling of an idealized kagome structure and are assumed to be frequency independent in the spectral range considered in this work.

The exponential loss rate (per m) of each mode and sideband is represented by $\alpha_{\sigma,l}$. For the fundamental mode these values were experimentally determined using a standard cut-back method, yielding values of the order a few dB/m.

Stimulated Raman scattering is seeded either by thermal phonons or by vacuum fluctuations at the Stokes frequency [5]. For simplicity in the simulations we assume a uniform noise floor of $E_{\text{noise}} = 50$ V/m for all the Raman lines and modes except the LP_{01} pump mode, a simplification that was successfully employed in a previous study [11].

With this, the spatiotemporal dynamics of the optical fields and the Raman coherence Q were modeled, and for simplicity only the LP_{01} and LP_{02} modes were included in the analysis. Nevertheless, the results are in remarkable agreement with experimental data [see Fig. 4(b)], the only free parameter being the attenuation of the LP_{02} mode at the Stokes frequency, which was taken to be 17 dB/m, a value in agreement with cut-back measurements of the LP_{02} mode loss for a similar kagome PCF [25].

The good agreement between theory and experiment allows the dynamics of the LP_{01} and LP_{02} Stokes modes to be investigated separately [Fig. 4(c)], as well as the intramodal and intermodal coherence Q [Fig. 4(d)]. The results show that the LP_{01} Stokes and anti-Stokes signals drop dramatically close to the gain suppression point [red solid line in Fig. 4(c)], while at the same time the LP_{02} signal [red dashed line in Fig. 4(c)] is enhanced. At large values of dephasing, in contrast, the LP_{02} signal is ~20 dB weaker than the LP_{01} signal, due to a lower spatial overlap and higher loss. Approaching the gain suppression point, the $LP_{01} - LP_{01}$ intramodal coherence drops strongly [Fig. 4(d)], while the $LP_{01} - LP_{02}$ intermodal coherence becomes dominant.

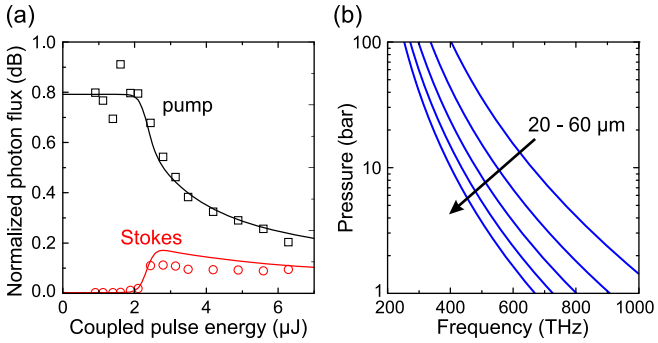

FIG. 5 (color online). (a) Pump and Stokes photon fluxes (normalized to the launched pump photon flux) plotted against pump energy at 24.5 bar. The measured data (squares and circles) are compared to the numerical results (solid lines). (b) Pressure-frequency dependence of the point of perfect gain suppression for five different core diameters between 20 and 60 μm. Different curves correspond to fibers with different hollow-core diameters.

As predicted in several papers [2–5] but never observed before in a collinear arrangement, the LP_{01} anti-Stokes signal peaks at two values of pressure above and below the gain suppression point. This is because the coherent phonons created by pump-to-Stokes conversion can immediately be used for pump-to-anti-Stokes conversion, even though slightly dephased. Nevertheless, conversion to the anti-Stokes frequency can be reasonably efficient (~1% in the experiment).

The conversion efficiency to the LP_{02} Stokes band peaked at 10% at a launched pump energy of 2.5 μJ and a pressure of 24.5 bar [see Fig. 5(a)], in good agreement with the numerical simulations. This peak arises because at high energy the Stokes light is generated close to the fiber input and is depleted by high LP_{02} loss, whereas at low energy the Raman gain is weak. As a result, for a given fiber length there is a pulse energy at which the conversion efficiency is maximum.

This falloff in conversion efficiency at high pump energies was already observed in the first demonstration of SRS in hydrogen-filled hollow-core PCF, although it was attributed to Raman-enhanced self-focusing [7]. Note that this phenomenon can be seen even if the pump wavelength and filling pressure do not fulfill the conditions for perfect gain suppression; indeed, both frequency and pressure ranges of gain suppression widen linearly with pump power. The pressures and optical frequencies for perfect gain suppression are plotted in Fig. 5(b) for core diameters between 20 and 60 μm.

In conclusion, gas-filled hollow-core kagome PCF provides a collinear system for observing the dramatic suppression of Raman gain first predicted by Bloembergen and Shen. This is achieved by operating in the vicinity of the pressure-tunable zero dispersion point, where at a specific

pressure and pump frequency the phonon coherence wave for pump-to-Stokes conversion exactly matches that for pump-to-anti-Stokes conversion. Suppression of Raman gain in a collinear system provides a route for investigating spontaneous Raman scattering at high pump energies, a regime that has so far been inaccessible because of the inevitable onset of SRS. Such studies may have important implications in quantum information, and lead to a deeper understanding of Raman scattering as a noise source in quantum optics, for example, in the generation of correlated photon pairs [26]. Strong suppression of LP_{01} Stokes amplification also allows high fidelity Raman amplification of higher order fiber modes [24], which is otherwise impaired by growth of the LP_{01} Stokes signal. This versatility in generating complex spatial light patterns at different frequencies could open new avenues for particle trapping and manipulation [27,28]. Moreover, if both pump and Stokes signals are simultaneously launched into the fiber, the collinear phase-matching scheme may lead to advances in highly sensitive coherent anti-Stokes Raman spectroscopy [29]. Finally, by tuning away from the point of perfect gain suppression, strong anti-Stokes bands can be generated, as predicted in 1964, but until now never exploited.

[1] R. W. Boyd, *Nonlinear Optics*, 3rd ed., (Academic Press, New York, 2008).
[2] N. Bloembergen and Y. R. Shen, Phys. Rev. Lett. **12**, 504 (1964).
[3] J. Herrmann, Sov. J. Quantum Electron. **5**, 207 (1975).
[4] S. Y. Kilin, Europhys. Lett. **5**, 419 (1988).
[5] C. Wu, M. G. Raymer, Y. Y. Wang, and F. Benabid, Phys. Rev. A **82**, 053834 (2010).
[6] M. D. Duncan, R. Mahon, J. Reintjes, and L. L. Tankersley, Opt. Lett. **11**, 803 (1986).
[7] F. Benabid, J. C. Knight, G. Antonopoulos, and P. St. J. Russell, Science **298**, 399 (2002).
[8] P. St. J. Russell, P. Holzer, W. Chang, A. Abdolvand, and J. C. Travers, Nat. Photonics **8**, 278 (2014).
[9] F. Couny, F. Benabid, and P. S. Light, Phys. Rev. Lett. **99**, 143903 (2007).
[10] S. T. Bauerschmidt, D. Novoa, B. M. Trabold, A. Abdolvand, and P. St. J. Russell, Opt. Express **22**, 20566 (2014).
[11] S. T. Bauerschmidt, D. Novoa, A. Abdolvand, and P. St. J. Russell, Optica **2**, 536 (2015).
[12] M. R. Sprague, P. S. Michelberger, T. F. M. Champion, D. G. England, J. Nunn, X.-M. Jin, W. S. Kolthammer, A. Abdolvand, P. St. J. Russell, and I. A. Walmsley, Nat. Photonics **8**, 287 (2014).
[13] F. Couny, F. Benabid, P. J. Roberts, P. S. Light, and M. G. Raymer, Science **318**, 1118 (2007).
[14] F. Belli, A. Abdolvand, W. Chang, J. C. Travers, and P. St. J. Russell, Optica **2**, 292 (2015).
[15] Y. R. Shen and N. Bloembergen, Phys. Rev. **137**, A1787 (1965).
[16] M. Finger, N. Y. Joly, T. Weiss, and P. St. J. Russell, Opt. Lett. **39**, 821 (2014).
[17] A. Rundquist, C. G. Durfee, Z. Chang, C. Herne, S. Backus, M. M. Murnane, and H. C. Kapteyn, Science **280**, 1412 (1998).
[18] E. Golovchenko, P. V. Mamyshev, A. N. Pilipetskii, and E. M. Dianov, IEEE J. Quantum Electron. **26**, 1815 (1990).
[19] F. Vanholsbeeck, P. Emplit, and S. Coen, Opt. Lett. **28**, 1960 (2003).
[20] T. Taru, J. Hou, and J. C. Knight, *European Conference and Exhibition on Optical Communication 2007* (VDE, Berlin, 2007).
[21] W. K. Bischel and M. J. Dyer, J. Opt. Soc. Am. B **3**, 677 (1986).
[22] M. G. Raymer and J. Mostowski, Phys. Rev. A **24**, 1980 (1981).
[23] G. P. Agrawal, *Nonlinear Fiber Optics*, 4th ed. (Academic Press, San Diego, 2007).
[24] B. M. Trabold, A. Abdolvand, T. G. Euser, A. M. Walser, and P. St. J. Russell, Opt. Lett. **38**, 600 (2013).
[25] B. M. Trabold, D. Novoa, A. Abdolvand, and P. St. J. Russell, Opt. Lett. **39**, 3736 (2014).
[26] A. S. Clark, M. J. Collins, A. C. Judge, E. C. Mägi, C. Xiong, and B. J. Eggleton, Opt. Express **20**, 16807 (2012).
[27] O. A. Schmidt, T. G. Euser, and P. St. J. Russell, Opt. Express **21**, 29383 (2013).
[28] A. Maimaiti, V. G. Truong, M. Sergides, I. Gusachenko, and S. Nic Chormaic, Sci. Rep. **5**, 9077 (2015).
[29] S. O. Konorov, A. B. Fedotov, A. M. Zheltikov, and R. B. Miles, J. Opt. Soc. Am. B **22**, 2049 (2005).